WEBER, P. and ERIC, R. H. Solid-state fluxed reduction of LG-6 chromite from the Bushveld Complex. *INFACON 6. Proceedings of the 6th International Ferroalloys Congress, Cape Town.* Volume 1. Johannesburg, SAIMM, 1992. pp. 71–77.

Solid-state Fluxed Reduction of LG-6 Chromite from the Bushveld Complex

P. WEBER and R. H. ERIC

University of the Witwatersrand, Johannesburg, South Africa

Carbothermic prereduction with cheap coal has gained importance as a means of improving the cost-effectiveness of ferrochromium production. The laboratory-scale study described in this paper was undertaken in order to investigate the influence of silica additions together with graphite and/or char on chromite reduction rates at different temperatures.

At lower temperatures (around 1300 °C), the addition of silica together with a graphite reductant did not promote the reduction of chromite. At higher temperatures (round 1500 °C), the addition of silica together with graphite resulted in a considerable enhancement of the reduction rate.

X-ray energy-dispersive analysis using a scanning electron microscope and X-ray-diffraction analyses proved the formation of a silica-slag phase in the presence of either silica or char, resulting in the agglomeration of the partly reduced chromite particles. The slag phase appeared to operate as a solvent for the components of the spinel. Metallization then took place by the reduction of the oxides (particularly chromium oxide) from the slag phase, resulting in the formation of mixed iron–chromium carbides.

Introduction

Over two-thirds of the energy consumed in conventional submerged-arc furnaces for the production of ferrochromium is used for heating and reducing chromite. In order to improve the cost-effectiveness, solid-state carbothermic prereduction with cheap coal prior to smelting has gained importance. A new prereduction process by which unagglomerated particles are reduced in a rotary kiln has recently been developed by Fried.Krupp GmbH[1]. The process is characterized by a higher operating temperature, the presence of a siliceous flux, and a large excess of reductant. The present laboratory-scale study was undertaken in order to investigate the fundamental mechanism and kinetics of silica-fluxed chromite reduction at temperatures in the range 1300 to 1500 °C.

Although numerous studies have been carried out on the reduction of chromite[2-7], information dealing with the enhancement of chromite reduction in the presence of fluxes is very incomplete. The two main studies that are quoted in this context are those of Kayayama[1] and Dawson[7].

Kayayama *et al.*[6] have shown that the reduction of chromite can be improved by the addition of chlorides such as NaCl and KCl, which act only by promoting the Boudouard reaction, and are therefore effective only at lower temperatures.

Dawson[7] investigated the mechanism and kinetics of promoted chromite reductions using several fluoride-based fluxes. Eutectic mixtures of NaF and CaF_2 were found to be particularly effective, even in small amounts. The flux acted as a solvent for the outer layer that consisted of a picrochromite–spinel solid solution, which was found to limit the reduction rate.

Experimental Procedure

Materials

The chromite ore used in this study came from the LG-6 seam of the Bushveld Complex. The chromite underwent washing and tabling in order to separate out gangue material. The chemical and screen analyses of the concentrated LG-6 ore are given in Table I. Graphite was mainly used as reductant, and was ground to a particle size of 0,038 mm. Additional experiments were conducted with char instead of graphite as reductant. The composition of the char used is shown in Table II. For silica addition, pure crystalline silica was used.

TABLE I
CHEMICAL AND SCREEN ANALYSIS OF LG-6 CHROMITE

Chemical analysis of LG-6 Ore								
	MgO	Al_2O_3	SiO_2	CaO	TiO_2	FeO	Fe_2O_3	Cr_2O_3
Mass %	9,32	15,12	<0,60	<0,20	0,67	19,85	6,73	44,21

Screen analysis of LG-6 ore			
Mesh size Tyler	Particle size mm	Distribution	Cumulative distribution %
48	0,295	5,65	94,35
65	0,208	5,94	88,41
100	0,147	15,80	72,61
150	0,104	33,33	39,82
200	0,074	27,39	11,88
270	0,053	8,98	2,90
400	0,037	1,89	1,05
	0,000	1,05	

TABLE II
CHEMICAL ANALYSES OF CHAR AND ASH

Chemical composition of char						
	C fix	Ash	Volatiles	Moisture	Phosphorus	Sulphur
Mass %	68,7	4,6	24,4	2,3	0,01	0,26

Chemical composition of ash							
	MgO	Al_2O_3	SiO_2	CaO	TiO_2	MnO	Fe_2O_3
Mass %	<0,30	27,10	47,30	2,30	1,28	<0,20	21,00

Experimental Set-up

The reduction of chromite was carried out in a molybdenum-wound thermogravimetric analysis furnace under an argon atmosphere. The reaction mixture consisted of chromite, reductant, and varying amounts of silica. The size of the silica particles was the same as that of the ore.

An alumina crucible containing these reaction mixtures was placed on a pedestal attached to a balance, and raised into the furnace. Mass loss was measured continuously, the data being stored on a PC and finally converted to reduction percentages:

$$R, \% = [\text{Mass of CO evolved}/((28/16)^* \text{ mass of original removable oxygen})] \times 100 \quad (1) \qquad [1]$$

For the calculation, only the chromium and iron oxides were regarded as reducible components.

After the experimental runs, the samples were separated and prepared for further evaluation by X-ray diffraction (XRD), by X-ray energy-dispersive analysis using a scanning electron microscope (SEM-EDAX), and by optical microscopy.

Experimental Results and Discussion

The first approach was to investigate the chromite reduction with and without silica addition at a relatively low temperature (1300 °C). Figure 1 shows the reduction curves obtained from mass-loss measurements at 1300°C with different amounts of silica, and with graphite as reductant. From these results, it is evident that the addition of silica did not enhance the reduction, even at additions of up to 7,5 per cent, which appeared to be the optimum addition. The final extent of reduction after 2 hours was only approximately 50 per cent and the reduction was still increasing.

SEM-EDAX work supported the conclusion that silica did not take part in the reduction at that temperature. Silica grains were detected unaltered next to the chromite grains after 2 hours of reduction (Figure 2). Fosterite formed only at very high silica additions, such as 10 per cent.

Further experiments were conducted with char as a reductant instead of graphite. Two findings were noted. Firstly, at 1300 °C, char did not enhance the reduction in comparison with graphite. Only in the initial state up to a reduction of about 20 per cent did char increase the reduction rate slightly due to its higher reactivity towards

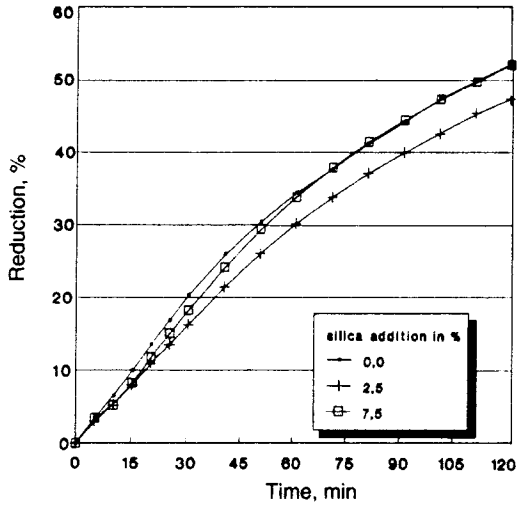

FIGURE 1. Effect of silica addition on reduction curves at 1300°C

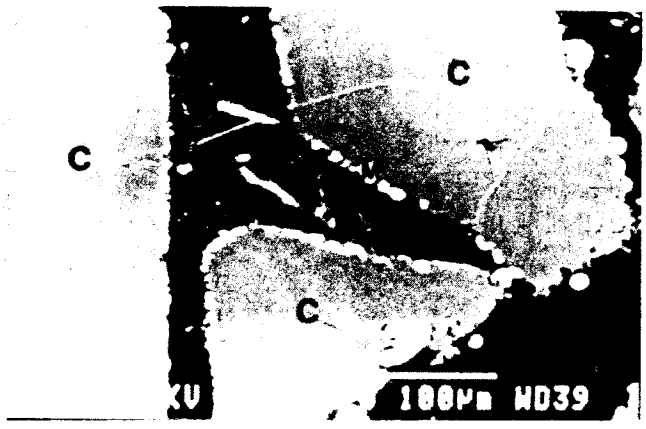

FIGURE 2. Secondary electron image of chromite particles reduced to 45 per cent at 1300°C in the presence of silica particles
C = Chromite S = Silica M = Metal

carbon dioxide. Secondly, the addition of extra silica to the char, as was done in the experiments carried out with graphite, did not promote the reduction.

Further testwork was carried out at 1500°C, aimed at the investigation of the possible effects of silica on chromite reduction with graphite as the reductant.

In contrast to the experiments conducted at 1300°C, silica addition appeared to have a positive effect on chromite reduction at 1500°C, as indicated in Figure 3. The extent of reduction was considerably increased by a silica addition of 7,5 per cent. The fact that more than 100 per cent reduction was achieved was due to the partial vaporization and reduction of oxides such as MgO, Al_2O_3, and SiO_2, which had been assumed to be non-reducible in the calculation. This explanation is supported by the finding of very small amounts of aluminium in the metal phase after the reduction, as well as pure recrystallized MgO at the top of the crucible. In fact, further condensation could occur outside the crucible and therefore would be responsible for an additional mass loss.

Furthermore, blank TGA runs were done using individually the reductant, the ore, and the mixture of SiO_2 and reductant. The results showed an extremely small mass loss for the SiO_2 and reductant mixture whereas, for the other blank runs, no mass loss was observed.

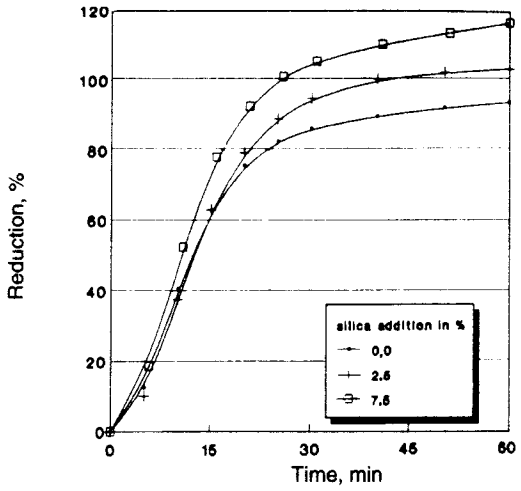

FIGURE 3. Effect of silica addition on reduction curves at 1500°C

Additional experiments were carried out with different particle sizes of ore and silica in order to investigate the influence of particle size. The results for a reduction at 1500°C, shown in Figure 4, indicate that a decrease in the particle size results in an increased rate of reduction and, more importantly, that the promoting effect of silica addition is enhanced with a decreasing particle size. Furthermore, it can be stated that the initial rate of reduction is not altered by any silica addition. The promoting effect of any silica addition on the rate of reduction becomes significant only at reduction levels exceeding approximately 80 per cent; at lower levels, the enhancement of the reduction with silica addition decreases to virtually zero.

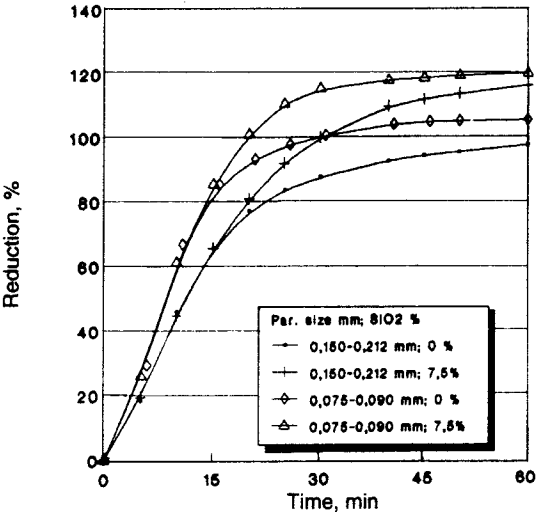

FIGURE 4. Effect of silica addition on the reduction of chromite at 1500°C in the particle-size range 0,150 to 0,212 mm and 0,075 to 0,090 mm

Experiments with char as reductant instead of graphite were also conducted. The final reduction rates achieved with char at 1500°C, as shown in Figure 5, matched those obtained with silica addition and a graphite reductant.

In order to simulate conditions in a rotary kiln, a stagewise reduction of chromite was conducted. Samples were first reduced for 2 hours at a temperature of 1300°C, and then for about 1 hour at 1500°C. The results show that the positive effect of silica addition becomes significant

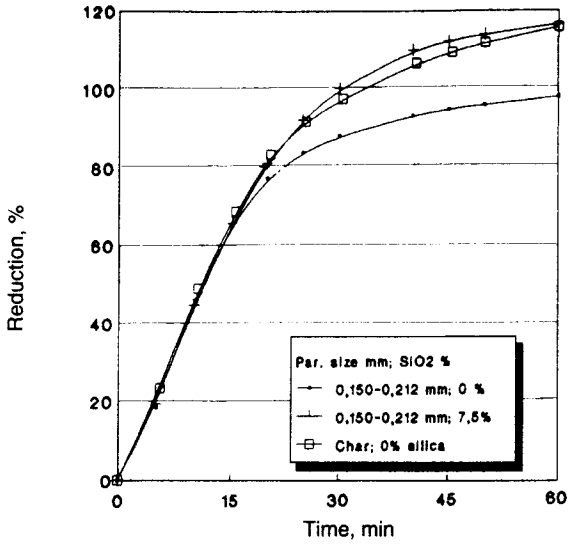

FIGURE 5. Effect of char on the reduction of chromite at 1500°C in the particle-size range 0,150 to 0,212 mm

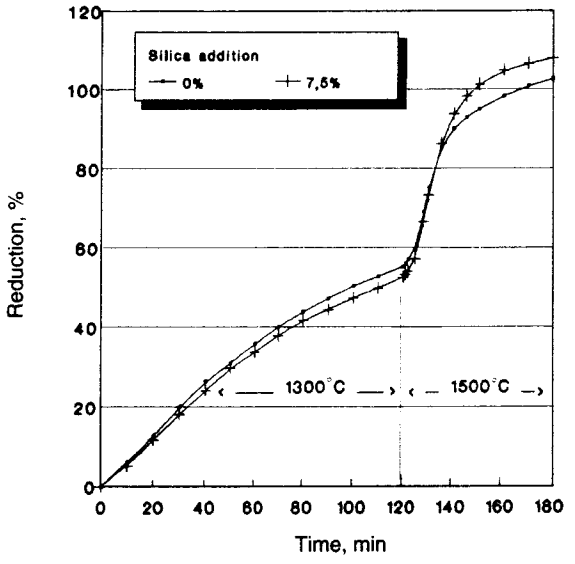

FIGURE 6. Effect of silica addition on a stagewise reduction

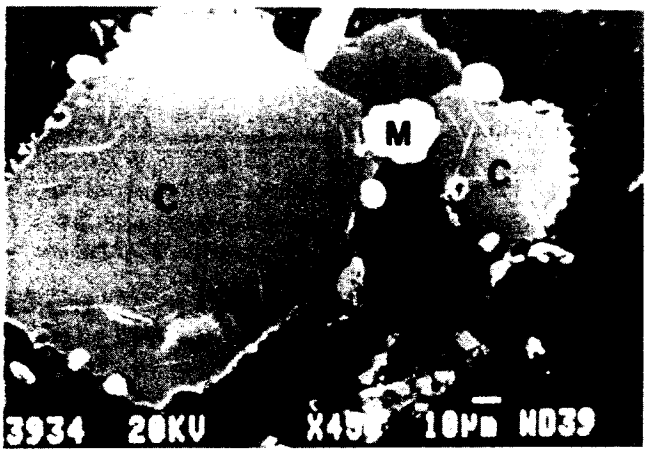

FIGURE 7. Secondary electron image of chromite particles reduced to 20 per cent at 1500°C in the presence of silica particles

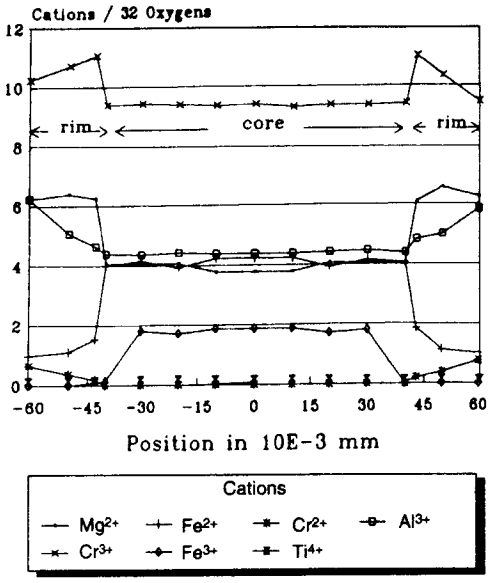

FIGURE 8. Variations in cations per 32 oxygen atoms across a particle that has undergone 20 per cent reduction

only at high temperatures (1500°C), similar to a non-stagewise reduction (Figure 6).

Furthermore, experiments were carried out with different retention times at 1500°C in order to investigate the reaction mechanism. For further evaluation of these data, XRD, SEM-EDAX investigations, and chemical analyses were carried out.

From SEM-EDAX work it was established that up to a reduction extent of about 30 per cent (approximately 6 minutes of reaction time), silica addition did not play a role in the reduction. Figure 7 shows chromite and silica grains adjacent to one another, revealing almost no alteration. Thus, during the initial stages of the reduction, silica has no effect on the reduction mechanism. An indication of the variation in cation distribution per 32 oxygen atoms across a chromite particle without silica addition (calculated on the assumption of a stoichiometric spinel structure as shown in the Addendum) is given in Figure 8. The cation distribution in Figure 8 does not change with any silica addition as silica is still not interfering with the chromite particles.

Obviously, the reaction starts with the reduction of Fe^{3+} to Fe^{2+} from the outside, resulting in the formation of an outer layer depleted in iron and an inner core consisting of the unaltered chromite represented by the formula

$$(Mg_{3,88}Fe_{4,12})[Al_{4,43}Cr_{9,43}Fe^{3+}_{1,81}Fe_{0,17}Ti_{0,17}]O_{32}.$$

In the outer layer all the Fe^{3+} is reduced to Fe^{2+} (since this reduction takes place at lower temperatures), and most of the Fe^{2+} was seen to be reduced to Fe° almost immediately, giving rise to a sharp gradient in Fe^{2+}. From the very small gradient of chromium across the particle, it can be deduced that hardly any chromium diffusion takes place.

In both cases, with and without silica addition, the initial metallization was in the form of iron, and carbides were found in the rim region. An increase in the chromium content was noted with continuing reduction.

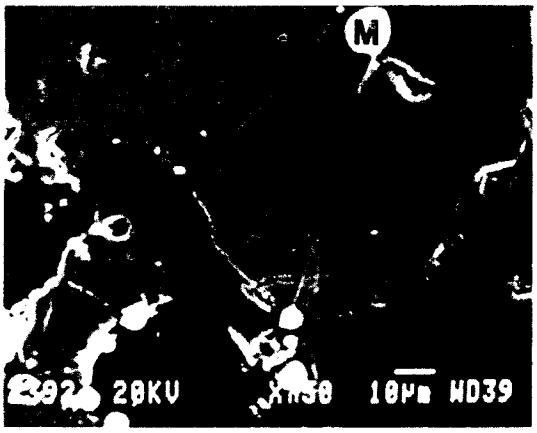

FIGURE 9. Secondary electron image of a silica-slag phase forming at the interface of a chromite particle reduced to 20 per cent
C = Chromite S = Silica M = Metal A = Slag

FIGURE 10. Secondary electron image of chromite particles embedded by a silica-slag phase after about 40 per cent reduction
C = Chromite S = Silica M = Metal A = Slag

The next step in the reaction sequence at 1500°C is very significant with regard to the influence of silica addition on the chromite reduction at this high temperature. In samples without silica addition, chromite grains became nearly completely depleted in iron as the unaltered core shrank, whereas samples with silica addition showed the additional formation of a silicate-slag phase at the grain edge.

Although the silicate-slag formation, as shown in Figure 9, can be observed at earlier stages of reduction such as 20 per cent, silica really influences the reduction reaction only at reduction levels exceeding 35 per cent, reacting at the interface of the distorted spinel to form a silicate-slag phase. This initial slag phase (Slag A in Table III) leads to an agglomeration of partly reduced chromite grains, as can be seen from Figure 10. The high chromium oxide content of this glassy slag phase reveals the fact that the spinel, and in particular its chromium oxide component, is being dissolved into the silicate slag.

Most of the chromium contained in the slag phase must be present in the divalent state, since former investigations[8,10] have shown that, at 1500°C , a low P_{O_2} and a high silica content lead to very high Cr^{2+}/Cr^{3+} ratios. This high Cr^{2+} content in the slag corresponds to the formation of a liquid slag phase, since previous studies[8,9] have proved a resulting decrease in the liquidus temperature of silicate slags with an increasing Cr^{2+} content.

A comparison of the variations in cation distribution per 32 oxygen atoms (again on the assumption of a stoichiometric spinel structure) for a sample after 35 per

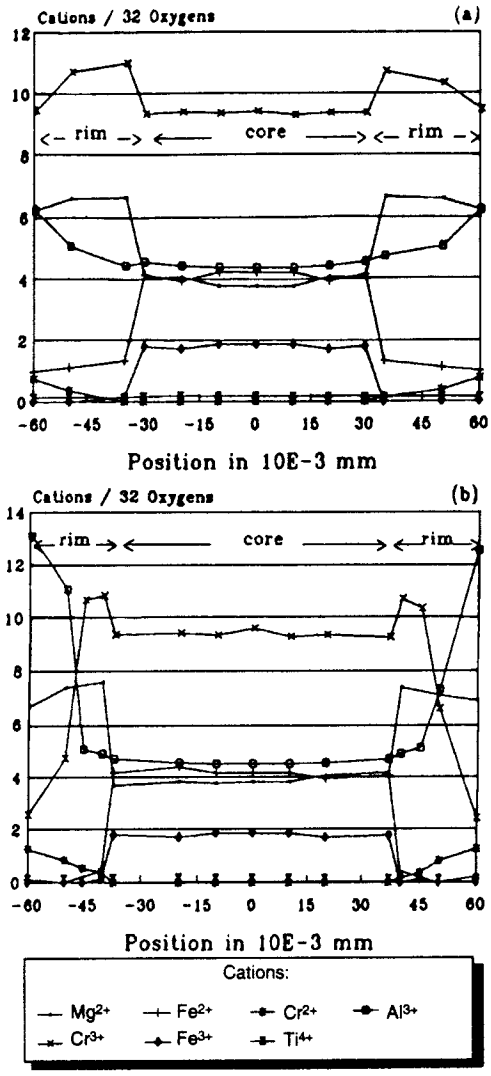

FIGURE 11. Variations in cations per 32 oxygen atoms across a particle
(a) reduced to 35 per cent without silica addition and
(b) reduced to 35 per cent with silica addition

cent reduction with and without silica addition is shown in Figure 11. While the remaining unaltered core is represented by the same spinel formula in both cases, the difference lies in the outer layer. In chromite grains without a silicate-slag formation, the distribution of Cr^{3+} cations is fairly homogeneous across the particle, and only at the immediate interface with the metal could a decrease in chromium cations be found. In the presence of a silicate slag, a gradient of Cr^{3+} cations proves that the chromium ions are diffusing out of the grain and into the silicate slag.

On the other hand, in order to maintain a spinel structure, an increase of Al^{3+} in the rim region occurs. Metallization of samples with silica addition at this stage occurs in the form of large blebs consisting of chromium and iron carbides mostly in the form of $(Fe,Cr)_7C_3$ embedded in the silica slag, as shown in Figure 10. These large metal blebs are characterized by a higher chromium content in comparison with the metal blebs found in samples reduced in the absence of silica. Considering the fact that the silicate slag is being depleted in chromium with further reduction, it is evident that metallization occurs by the reduction of chromium from the slag phase.

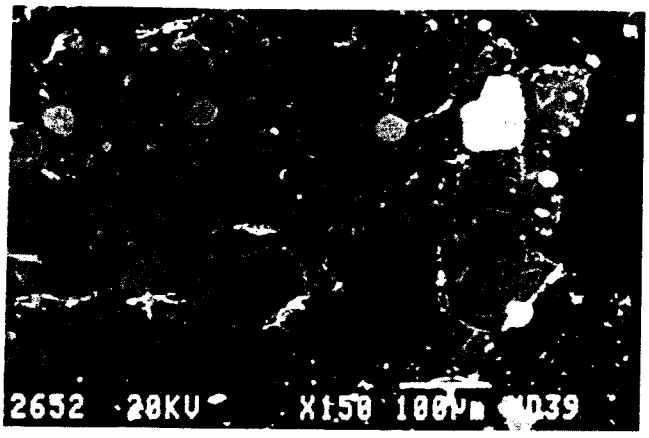

FIGURE 12. Secondary electron image of chromite-particle agglomeration after about 60 per cent reduction

TABLE III
CHEMICAL COMPOSITION OF SILICA SLAGS

Slag	Slag A after 35% reduction mass %	Slag B after 80% reduction mass %	Slag C after 35% reduction mass %	Slag D after 80% reduction mass %
SiO_2	57	55	40	54
Al_2O_3	23	24	25	18
CrO	14	4	16	6
MgO	4	12	15	16
TiO_2	1	1	1	1 – 2
CaO	0	0	1 – 2	1 – 2

In comparison, Figure 12 shows small amounts of metal phase formed in the altered and distorted spinel, which result from a change in morphology causing metallization inside the chromite grain. These metal blebs are still enriched in iron and depleted in chromium, which is further evidence that most of the chromium metallization occurs by chromium reduction via the slag phase to form metal blebs located in the slag phase.

With further reduction, metallization of chromium continues, with the slag phase becoming more and more depleted in chromium and enriched in magnesia. A typical slag composition after about 80 per cent reduction is shown as Slag B in Table III. The change in composition with the limited solubility of components leads to a recrystallization of both an alumina–magnesia spinel containing low amounts of chromium and a fosterite phase. As a result, the amount of slag phase present decreases with continuing reduction.

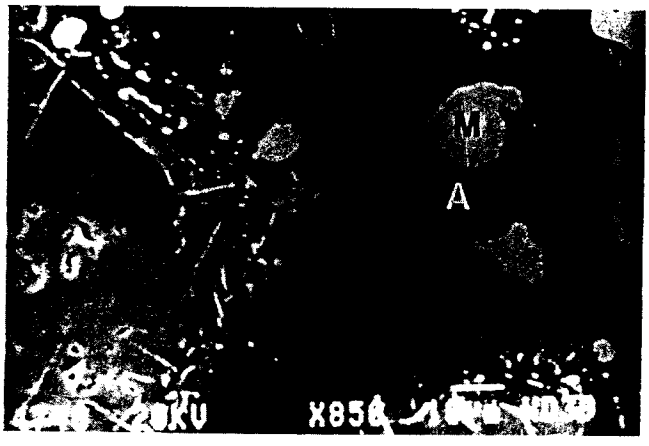

FIGURE 13. Secondary electron image of chromite particles reduced with char to 35 per cent
C = Chromite M = Metal A = Slag

It is of further interest to examine the influence of char on the reaction mechanism. As shown in Figure 13, a similar slag formation was found at even lower reduction percentages containing more calcium oxide, as shown in the analysis of Slag C in Table III. This slag formation was attributed to the ash resulting from the char addition. The higher calcium oxide content of the ash shown in Table II is thought to cause the higher calcium-oxide content of the slag. The SEM photomicrographs further show a dissolution of the spinel components. The composition of Slag D after 80 per cent reduction with char indicates that chromium is reduced from the slag phase in a similar way to that in which it is reduced with graphite in the presence of silica. Recrystallization of fosterite and magnesia–alumina spinel was also found.

Conclusions

Laboratory-scale investigations have shown that, at 1500 °C, silica flux enhances the chromite-reduction reaction. SEM-EDAX work has shown the formation of silicate slag, which tends to agglomerate the partly reduced chromite particles. The slag phase operates as a solvent for the spinel components, particularly chromium oxide, which are then reduced or recrystallized out of the slag. When char is used as a reductant, similar results are obtained, since its ash composition leads to the formation of a silicate-slag phase. The formation of a silicate-slag phase results only in an improvement of the reduction rate during the final stages of reduction, when further reduction of the chromite without silica addition is retarded by its refractory properties.

Acknowledgments

This paper is published by permission of Mintek, and the Ferro Alloy Producers' Association of South Africa. The authors are deeply grateful to both these organizations for their financial support.

References

1. Fried. Krupp GmbH. (1984) Process for the production of ferrochromium. *S.Afr. pat.* 8 410 101.
2. Perry, K.P.D. (1986). Thermodynamical analysis of the reduction of chromites. PhD thesis, University of the Witwatersrand, Johannesburg.
3. Rankin, W.J. (1978). Solid state reduction by graphite and carbon monoxide of chromite from the Bushveld Complex. *Report* 1957, NIM, Randburg.
4. Searle, M.J. (1984). The combined prereduction of UG-2 chromite and Thabazimbi haematite. PhD thesis, University of the Witwatersrand, Johannesburg.
5. Soykan, O. (1988). The solid state reduction characteristics of the Bushveld Complex chromites. PhD thesis, University of the Witwatersrand, Johannesburg.

6. Kayayama, H.G., Tokuda, M., and Othani, M. (1982). Promotion of carbothermic reduction of chromium ore by the addition of borates. *Trans. Iron Steel Inst., Japan*, 22, (2), p. B37.
7. Dawson N.F. (1985). Factors affecting the reduction rate of chromite. PhD thesis, University of Natal, Durban.
8. Tsai, H.T. (1981). Slag–metal refractory equilibria of chromium containing phases in steelmaking. PhD thesis, Pennsylvania State University.
9. Rennie, M.S. (1972). The effects of chromium oxide, iron oxide and calcium oxide on the liquidus temperatures, viscosities and electrical conductivities of slags in the system $MgO–Al_2O_3–SiO_2$. PhD thesis, University of the Witwatersrand, Johannesburg.
10. Pretorius, E.B. Private communication, Mintek, Randburg.

Addendum: Calculation of Cations

The sample represents the unreduced core of a chromite grain. The mass percentages from SEM-EDAX are converted into atomic fraction as follows:

Element	Mg	Fe	Al	Cr	Ti	O
Mass %	5,86	21,75	7,19	31,652	0,55	33,03
N_i	0,07	0,11	0,08	0,17	0,003	0,58

The numbers of cations per 32 oxygen atoms are calculated as follows:

N_{Mg}/N_O * 32	=	3,86	Norm to 24	=	3,88
N_{Fe}/N_O * 32	=	6,07		=	6,10
N_{Al}/N_O * 32	=	4,43		=	4,43
N_{Cr}/N_O * 32	=	9,38		=	9,43
N_{Ti}/N_O * 32	=	0,17		=	0,17
Total:		23,89			24,00

Normalization became necessary since it is assumed that, for a spinel structure, 8 tetrahedral and 16 octahedral sites are occupied by cations. Since Ti^{4+} forms ulvospinel with Fe^{2+}, the spinel structure will be expressed as

Fe^{2+} in octahedral sites = 0,17
Fe^{3+} in octahedral sites = [(6,10-0,17) + 8 = 1,81
Fe^{2+} in tetrahedral sites = [6,10 – 0,17 + 1,81 = 4,12
Mg^{2+} in tetrahedral sites = 3,88
Al^{3+} in octahedral sites = 4,43
Cr^{3+} in octahedral sites = 9,43·

Hence, the spinel can be expressed by the following chemical formula:

$$(Mg_{3,88}Fe_{4,12})\,[Al_{4,43}Cr_{9,43}Fe^{3+}_{1,81}Fe^{2+}_{0,17}Ti_{0,17}]O_{32}\cdot$$